



Western Michigan University
ScholarWorks at WMU

Honors Theses

Lee Honors College

4-12-2018

The Proton Veto Project at WMU/MSU

Justin Swaim

Western Michigan University, officialswaim@gmail.com

Follow this and additional works at: https://scholarworks.wmich.edu/honors_theses



Part of the Physics Commons

Recommended Citation

Swaim, Justin, "The Proton Veto Project at WMU/MSU" (2018). *Honors Theses*. 2970.
https://scholarworks.wmich.edu/honors_theses/2970

This Honors Thesis-Open Access is brought to you for free and open access by the Lee Honors College at ScholarWorks at WMU. It has been accepted for inclusion in Honors Theses by an authorized administrator of ScholarWorks at WMU. For more information, please contact wmu-scholarworks@wmich.edu.



**The Proton Veto Project at Western Michigan
University/Michigan State University**

Justin Swaim

Lee Honors College

Western Michigan University

Department of Physics

Thesis Mentor: Dr. Zbigniew Chajecki

Thesis Committee:

Dr. Zbigniew Chajecki

Dr. Michael Famiano

Abstract

The Proton Veto Wall (VW) is a charged particle detector designed and built at Western Michigan University for use at the National Superconducting Cyclotron Laboratory at Michigan State University. The VW assists the Large Area Neutron Array (LANA) with discriminating between charged particles detected via proton recoil in the scintillating material and charged particles detected from heavy ion collisions produced in the laboratory. Twenty five Eljen-200 plastic organic scintillators are arranged in a vertical position with photomultiplier tubes (PMTs) mounted to either end. The detector sits directly in front of LANA on a large stand that was assembled using T-slotted frames. Whenever a charged particle interacts with the scintillating material, photons are produced in a process known as fluorescence. Their energy is directly proportional to the energy deposited by the charged particle. Photomultiplier tubes gather these photons and external laboratory electronics process the signals produced in the PMTs. To understand how these signals relate back to the energy of the charged particle, the VW was calibrated using gamma sources. Two types of calibrations took place: energy calibrations and time calibrations. Time calibrations allow the position of the charged particle to be determined as a function of time. Once the charged particle location is known in the VW it is consequently known in the LANA and its signal is ignored by LANA. The VW successfully vetoes over billions of charged particle signatures from the LANA while keeping track of the energy of charged particles as they pass through the VW.

Heavy Ion Collisions

Neutron stars are extremely dense celestial objects that form when massive stars collapse and explode; leaving behind only the matter that was compressed during the collapse [Hoyle]. Due to their distance from Earth, neutron stars are difficult to observe and impossible to perform experiments on. In order to access the physics behind neutron stars, experimental nuclear physicists need to find suitable models that can be experimented on in the laboratory setting. One such way of accessing the physics behind neutron stars is by colliding heavy nuclei. When heavy nuclei collide a high density nuclear matter (similar to that of neutron stars) is created. Then, the nuclei break apart and emit particles (such as protons and neutrons) and other light elements (such as e.g. Helium-4 and deuteron). The dependence of the symmetry energy on the density of nuclear matter can be studied by varying the incident energies and impact parameters [Danielewicz]. The Proton Veto Wall is used with other detectors at the National Superconducting Cyclotron Laboratory to study heavy ion collisions and allow parallels to be drawn to what happens in neutron stars.

Introduction to Particle Detection

One of the main focuses of nuclear physics is on the interactions that occur between nuclei. To detect, monitor, and identify what occurs during these reactions, a particle detector must be used. Particle detectors are used to gather information about the nuclear collisions such as time of flight and energy of the particles emitted. For some detection methods this means that the particle can deposit all of its energy by stopping in the material or only deposit a fraction of its energy by scattering off of the material. In scintillation detection, particles that interact with the scintillating

material can deposit energy by scattering from the atoms that make up the material [Knoll, 229]. When scattering occurs, electrons bound to the scintillator's atoms are knocked out of their ground energy state and are excited to some higher energy state. Electrons return to ground state by releasing energy in the form of electromagnetic radiation, or light [Taylor]. These photons (light particles), have discrete wavelengths and energies that are directly proportional to the energy that was deposited by the incident particle [Knoll, 231]. The process by which energy is released in the form of light is known as fluorescence and is illustrated in figure 1.

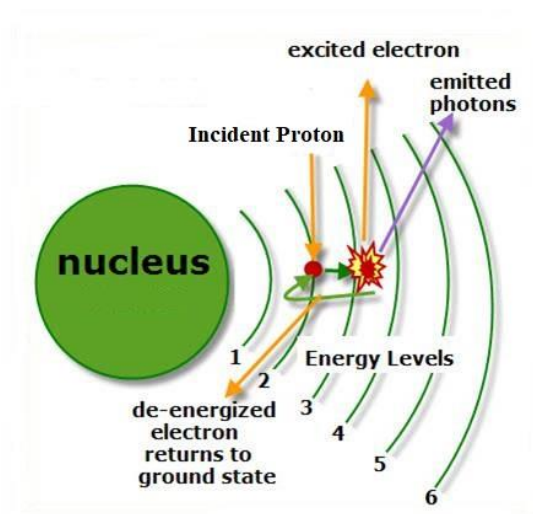


Figure 1 A diagram showing the fluorescence process that occurs when electrons are excited and then return to ground state [Vancleave, 2011].

At the National Superconducting Cyclotron Laboratory (NSCL) at Michigan State University (MSU) neutron detection is carried out using the Large Area Neutron Array (LANA), also known as the neutron wall (NW) shown in figure 2. The NW determines the energy of incident neutron particles by measuring the energy of the recoiled protons from the nuclear reaction [Knoll, 569-575] [Coupland].

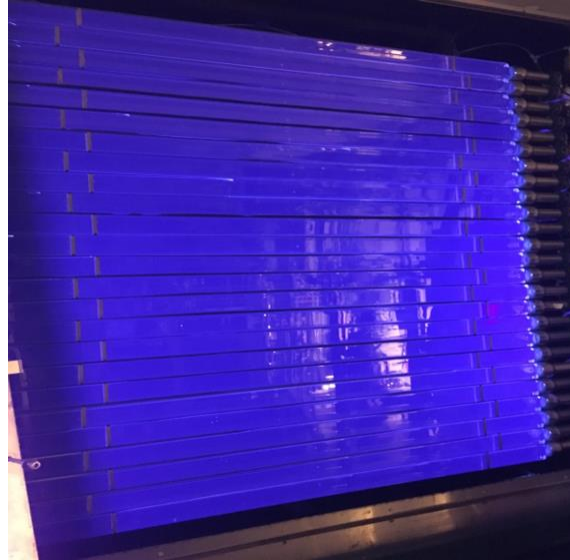


Figure 2 The Large Area Neutron Array (LANA) at NSCL. It is fluorescing because it has been exposed to an ultra violet source.

Because the NW relies on the charge of the recoil proton to predict neutron energy, the NW will also measure any proton that strikes its surface; allowing it to detect both neutrons and protons but leaving it unable to discriminate between the two as they interact with the detector [Coupland]. A second detector was designed and built at Western Michigan University to sit in front of the NW that allowed discrimination between neutrons and protons. This second detector, called the Proton Veto Wall (VW), is able to determine when a charged particle has passed through it and, using position sensing, is able to tell the NW where the charged particle will strike. This allows the NW to veto, or cancel, any attempt to record information produced by the charged particle signal. The VW will extend the lifetime and the efficiency of the NW at NSCL by fulfilling a much needed role in charged particle discrimination, allowing for a variety of new experiments to be conducted and improving the overall accuracy of these experiments.

Construction of the Proton Veto Wall

The Proton Veto Wall is comprised of 25 vertical Eljen-200 plastic organic scintillators arranged in a “staggered” position that allows the scintillators to overlap, forming a solid wall for charged particle detection (see figures 3 and 4). Each of the scintillators is 2.5 meters in height, 1 centimeter in thickness, and 9.4 centimeters wide. Both ends of the scintillator narrow by an angle of 80.66 degrees to form a final width of 5.65 centimeters that allows the scintillator to be coupled to a light guide. The scintillators are first wrapped in a black paper and then in black vinyl to prevent outside light from entering the system. The scintillator bars are attached to a 1.9 centimeter thick cylindrical light guide that is 7.5 centimeters in diameter. The design of the light guide incorporates a cavity that allows the scintillator bar to “slot” into it and is filled with Eljen-500 epoxy to maintain coupling and allow smooth light transmission across the interface (figure 7). The light guide assembly is attached to an Amperex XP3462 photomultiplier tube (PMT) using Sylgard 184 Silicon Elastomer. The top 5 centimeters of the Amperex PMT are coated with Eljen-510 reflective paint and the light guide/PMT assembly is covered in the same black paper and vinyl as the scintillator bars in order to prevent outside light from entering the sides of the PMT (figure 8). A 3D printed plastic ring is mounted to the outside of the light guide that allows a metallic shield to be placed around the PMT. This shielding prevents magnetic fields from entering the PMT and interfering with the electric fields it uses to guide electrons during the multiplication process (see “creating a signal using photomultiplier tubes” for more information about PMT function).

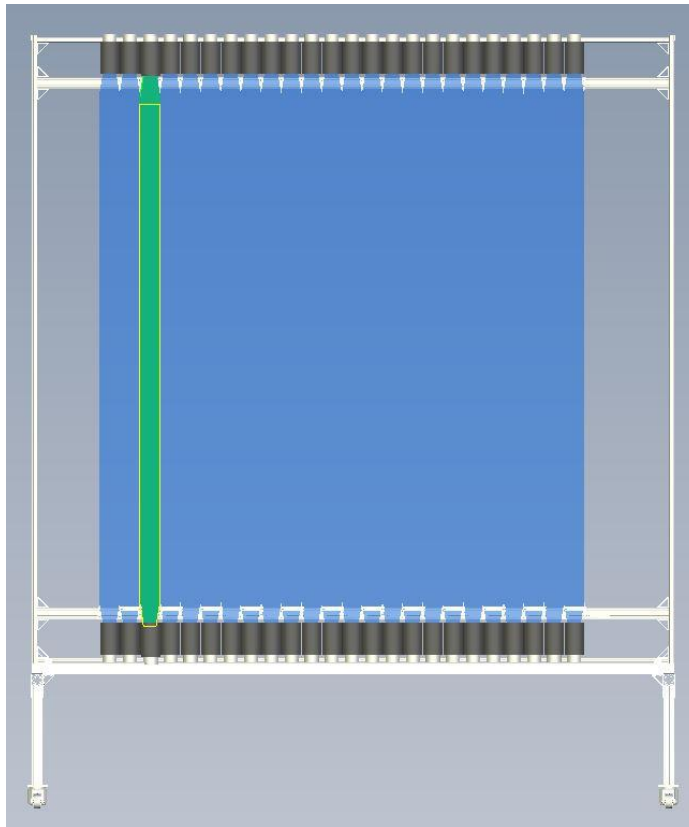


Figure 3 A schematic diagram of the Proton Veto Wall. One scintillator bar is highlighted (in green). The scintillator bars are arranged vertically, which is in contrast to the horizontal position of LANA's orientation shown in figure 2.



Figure 4 The Proton Veto Wall. It is the black vertical bars that the flag covers, in the background. Justin Swaim is pictured in the foreground of the photo. The detector itself is about 3 meters in height, and is situated in front of LANA (metal shielded surface behind the black scintillator bars).

Integration with the Neutron Wall at NSCL

The frame holding the Proton Veto Wall is designed to rest against the Neutron Wall at NSCL. This allows experimenters to adjust the coverage of the VW and place the VW bars as close to the NW detector as possible (figure 5). The entire frame was constructed and built using T-slotted framing at WMU. The bottom of the framing system is built similarly to a table, with a wheel/brake system on each leg that allows the frame to be rotated and positioned directly in front of the NW. The rest of the frame sits atop this table and perpendicular to its face. Due to its close proximity to the NW, the VW is able to give an accurate approximation of where a charged particle will land on the NW so its information can be vetoed.

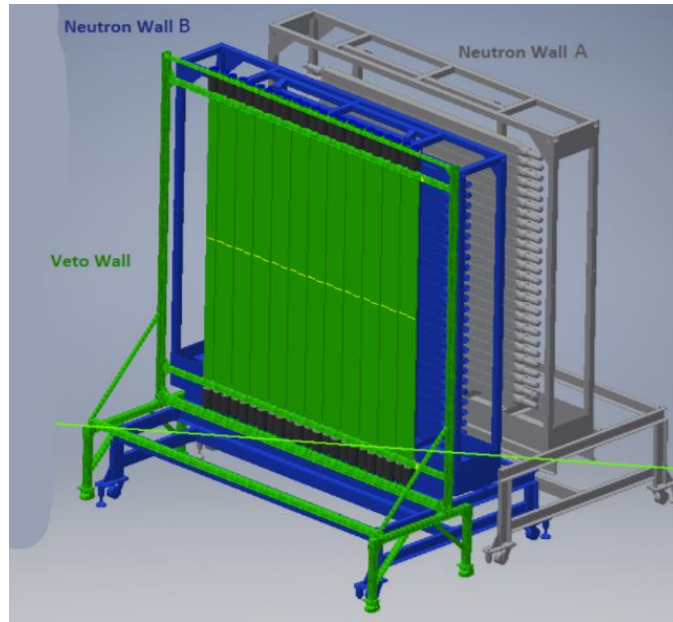


Figure 5 The experimental setup of the Large Area Neutron Array and Proton Wall. In the foreground (green) is the VW. The first NW lies behind it (blue) and the second NW is in the far back (grey).

Operating Principles of the Veto Wall

During a heavy ion collision the two colliding nuclei break up into neutrons, protons, and lighter elements such as deuteron, Helium-3, Helium-4, etc [Danielewicz]. As these particles travel from the reaction chamber to the detectors, they must cross some well-defined distance. Those particles have kinetic energy that they can deposit into the materials they pass through, including the VW. Because neutrons have, in general, a small cross section on interaction with most materials, it is unlikely they will interact with the VW [Knoll, 55]. This means that only charged particles will scatter from the scintillating material. When scattering occurs, charged particles impart some of their kinetic energy to electrons in the scintillating material's atoms by colliding and reflecting off of them at some angle. Electrons that are bound closely to the nucleus of the atom have a very low energy, and therefore are easy to free, while electrons farther from the nucleus have a very high

energy, and are therefore more difficult to release from their orbitals. Regardless of its proximity to the nucleus, once the electron is freed from its shell, a “hole” is left in the electron shell that needs to be filled [Taylor]. Electrons are naturally attracted to the positively charged nucleus of the atom, so an electron that was excited to a higher energy state will lower back to its original state closer to the nucleus. As the electron returns to its ground state, it releases energy in the form of light in a process known as fluorescence (see figure 1). The photons are later converted to electrons that allow the energy given off by the collision to be measured by external signal processing electronics. The number of photons produced by the fluorescence process is directly proportional to the energy deposited by the charged particle during collision [Knoll, 231]. The analysis of these photons is what allows the VW to determine the energy of the incident charged particles and the position of the charged particle as it passes through the detector.

Creating a Signal Using Photomultiplier Tubes

Scintillation is a broad term that refers to the process of light emission. In the Eljen-200 organic plastic scintillators, the scintillating material is especially made so that whenever particles interact with it, electrons from the orbital shells of the scintillators atoms are easily excited. This excitation process occurs whenever particles released from the reaction chamber interact with the VW. During the scattering process, bound electrons move from a ground state to a higher, more excited state. As they return to their ground state these electrons give off light in the form of photons during a process called fluorescence (a fluorescing scintillator bar is shown in figure 6) [Knoll, 223].

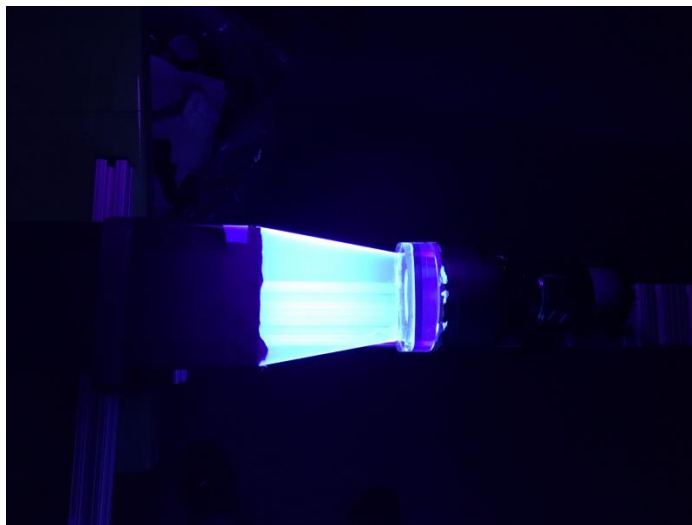


Figure 6 A small section of the scintillator bar is exposed to UV light while undergoing repairs.

Emitted photons are collected in the photomultiplier tubes at each end of the scintillator. In order to recover as much light at the maximum energy possible, the Eljen-200 material is smooth and transparent and has no cracks or unnecessary surfaces to minimize the reflection of the light. In addition, the scintillator detectors are wrapped in black paper and vinyl to prevent light from outside sources reaching the PMTs (figure 8). Outside light could produce signals in the PMT that are stronger than the signals produced by charged particles. In addition to its previous benefits, the vinyl tape also absorbs photons that reflect from inside the scintillator in order to keep photons from reflecting multiple times and losing energy; this would worsen the time resolution of the detector. Each PMT (with the exception of its interface) was painted with highly reflective paint before they were covered with black paper and vinyl. The interfaces (where light guide, PMT, and scintillator meet) utilize special epoxies (Sylgard 184 and Eljen-500) that combine the materials without providing a change in the refractive index (~ 1.5) [Knoll, 223]. These epoxies prevent photons from losing energy as they move through different materials.

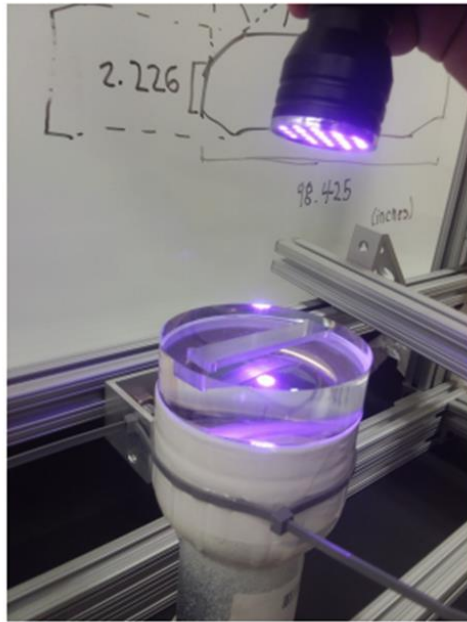


Figure 7. The top of a PMT is exposed to UV light, allowing a better view of the plastic light guide that sits atop it (clear cylinder with slot).



Figure 8. The finished product of the process that makes the scintillators "light tight". After having been painted in reflective paint, it is then wrapped in black vinyl as seen in the picture.

The conversion of photons to electrons occurs at the photocathode of the PMT. Here, a photo emissive material allows electrons to be released whenever photons, such as the photons released by charged particles, interact with it (via the photoelectric effect). Newly generated electrons are then directed into the vacuum space of the PMT, where a focusing grid will provide an electric field that directs the electrons to a dynode. Dynodes are metal surfaces that provide an excess of

electrons. Whenever a charged particle (such as the electrons emitted from the photocathode) strikes the dynode, more electrons will then be released. This process, called secondary emission [Knoll, 41], allows the total number of electrons available in the PMT to be multiplied by a certain factor [Scintillation Detectors]. Multiplication can happen several times, and the Amperex XP3462 is an 8 stage multiplier, meaning multiplication happens 8 times. Each dynode is maintained at a positive electrical potential that is higher than the previous and are specifically positioned to direct electrons to the next dynode. The supply voltage of the PMT determines how many electrons are emitted at the dynodes (also known as the gain factor). Once the multiplication process is finished, the electrons gather at the anode and a current is produced at the output [Scintillators]. Because of the varying number of PMTs, each scintillator needs to have its PMTs calibrated to unique bias voltages in order to match the spectra produced when charged particles deposit energy in the VW [Prekeges]. To prevent magnetic fields from interfering with the electric field inside the PMT, a special metallic shield encloses the device. An illustration of the inner workings of the PMT is shown below in figure 9.

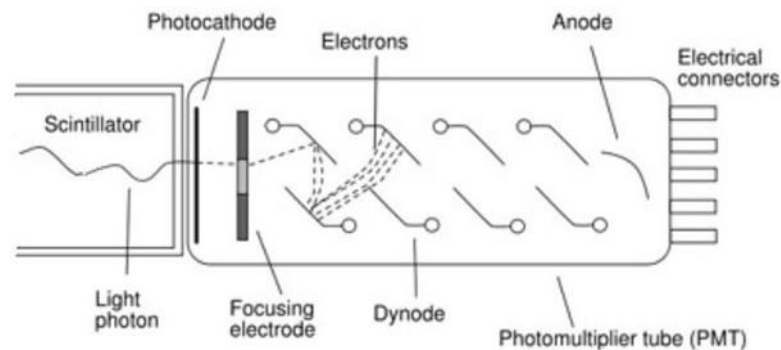


Figure 9. A schematic diagram that shows the multiplication process that occurs in the photomultiplier tubes [Scintillators, 2009].

Energy Calibration

The relationship between radiation energy deposited in the detector by a charged particle and the signal it generates in the photomultiplier tubes can only be determined after the Proton Veto Wall has been calibrated. Calibrations were performed using three gamma sources: Cobalt-60, Cesium-137, and Manganese-54 (figure 10 shows the Co-60 sample). An example of the uncalibrated gamma energy spectrum for Co-60 is shown in figure 11. In that example, the location of the Compton edge is shown (in purple); figure 12 takes a closer look at this region of the gamma spectrum. When these sources undergo gamma decay, each releases a gamma particle with a unique and a well-known energy (1333, 662, and 835 keV respectively) [Knoll, 455]. Moving the position of the gamma sources up and down the scintillator bar changes the signal generated in the PMTs by the photons.



Figure 10 The Co-60 gamma source used in the calibration process.

Energy deposited by the gamma particles depends on the angle at which they strike the VW. Since the kinetic energy and momentum of two bodies colliding is conserved, a simple rearrangement of

kinematics yields Compton's Formula. This formula allows the energy of the scattered charged particles or gamma particles to be computed for various scattering angles [Knoll, 323-325]:

$$\frac{1}{E'} - \frac{1}{E_0} = \frac{1}{m_e * c^2} * (1 - \cos(\theta))$$

Here, θ is the scattering angle, E_0 is incident charged particle or gamma particle energy, E' is the energy of the particle after it scatters (energy after impact), and the difference between the two, $E_0 - E'$, is the energy deposited in the detector at the specific angle. The variation in theta, the scattering angle, and deposited energy creates an energy spectrum that displays a wide range of energies (figure 11). Table 1 shows tabulated values for Compton's Formula for each of the three gamma sources when the scattering angle is equal to 180 degrees what corresponds to the maximum energy deposited by the particle in the scintillator.

Table 1 Tabulated values for Compton's Formula when theta = 180 degrees for each of the three gamma sources.

	E_0 (incident energy)	E' (scattered energy)	$E_0 - E'$ (deposited energy)
Co-60	1333	214	1119
Mn-54	835	196	639
Cs-137	662	184	478

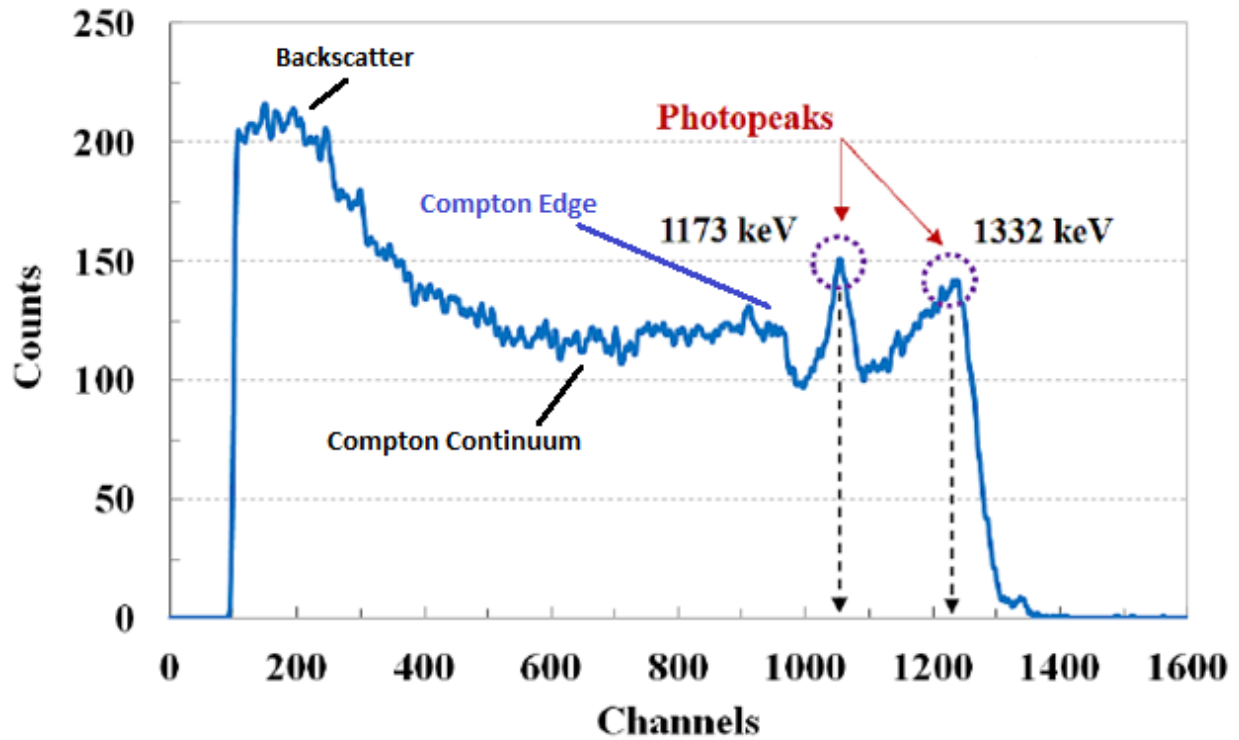


Figure 11 Uncalibrated gamma-ray energy spectrum for Co-60 [Yoo, 2015]

At the far end of the spectra lies the Compton Edge (CE); a feature of the spectra that shows the maximum amount of energy deposited when the scattering angle is equal to 180° . The unique shape of the energy spectra allows a Gaussian distribution to be fit to the curve so that the CE can be calculated. From the Gaussian distribution, a function can be generated that provides the location of the CE at the half max half width of the right hand side of the distribution (marked in green in figure 12).

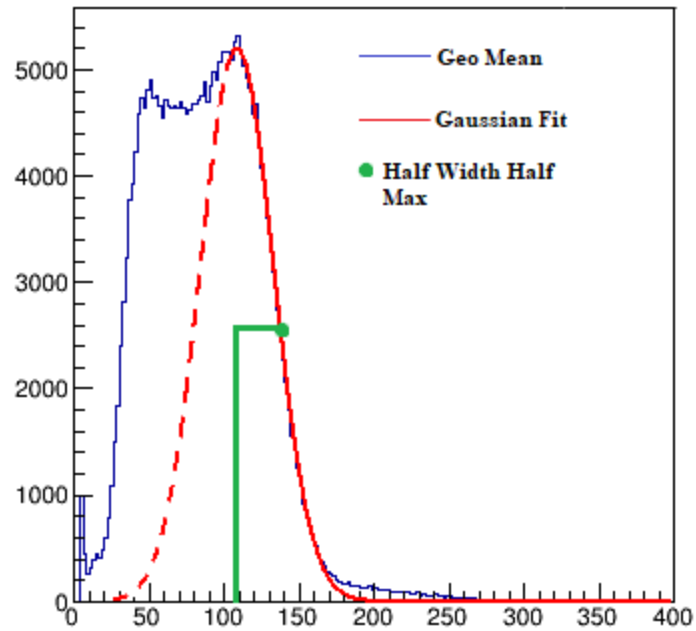


Figure 12 An example output showing how the Gaussian distribution (red) is fit over the energy spectra (blue) to yield the location of the Compton Edge at the half max half width of the peak.

Once the CE for the spectra of each source at a particular position has been found the relationship between energy deposited into the detector and the channel number can be determined.

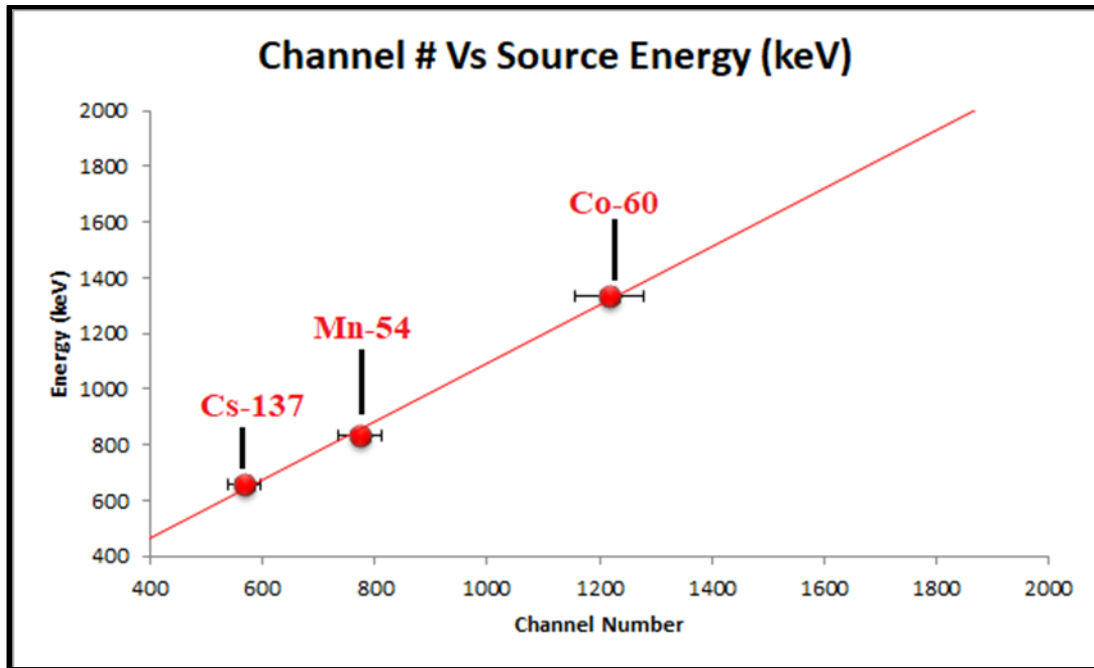


Figure 13 A rough approximation of the linear relationship between channel number and source energy. Here, Cs-137 is the point on the left, Mn-54 is in the middle, and Co-60 is on the far right.

An example of an energy calibration is shown in figure 13. The energy deposited by a particle into the VW relates the channel number it is placed in to the energy which represents that channel number (determined beforehand using the energy calibration).

Timing Calibration

Timing calibrations were performed to determine the time it takes for photons to travel through the scintillating material. Similar to the energy calibrations, each gamma source was placed at varying positions on the scintillator bars to find the relation between the time it took for deposited energy to reach the photomultiplier tubes and the timing signal it generated in the PMTs. Each PMT shares the same start time but has a different stop time because the time it takes the photons to reach either PMT depends on where the charged particle landed on the scintillator bar. For one

particular set of timing calibrations, the gamma sources were placed 20 centimeters away from the top and bottom PMTs. When the gamma sources were placed close to the top of the scintillator, the timing signals arrived much sooner to the top PMT than the bottom PMT. The reverse was true when the sources were placed on the bottom of the scintillator bars. When the difference between the two timing signals is computed (time to top PMT minus time to bottom PMT) for both cases (when the source is on the top and bottom of the scintillator bar) the timing information can be used to generate a function of position based on the time difference.

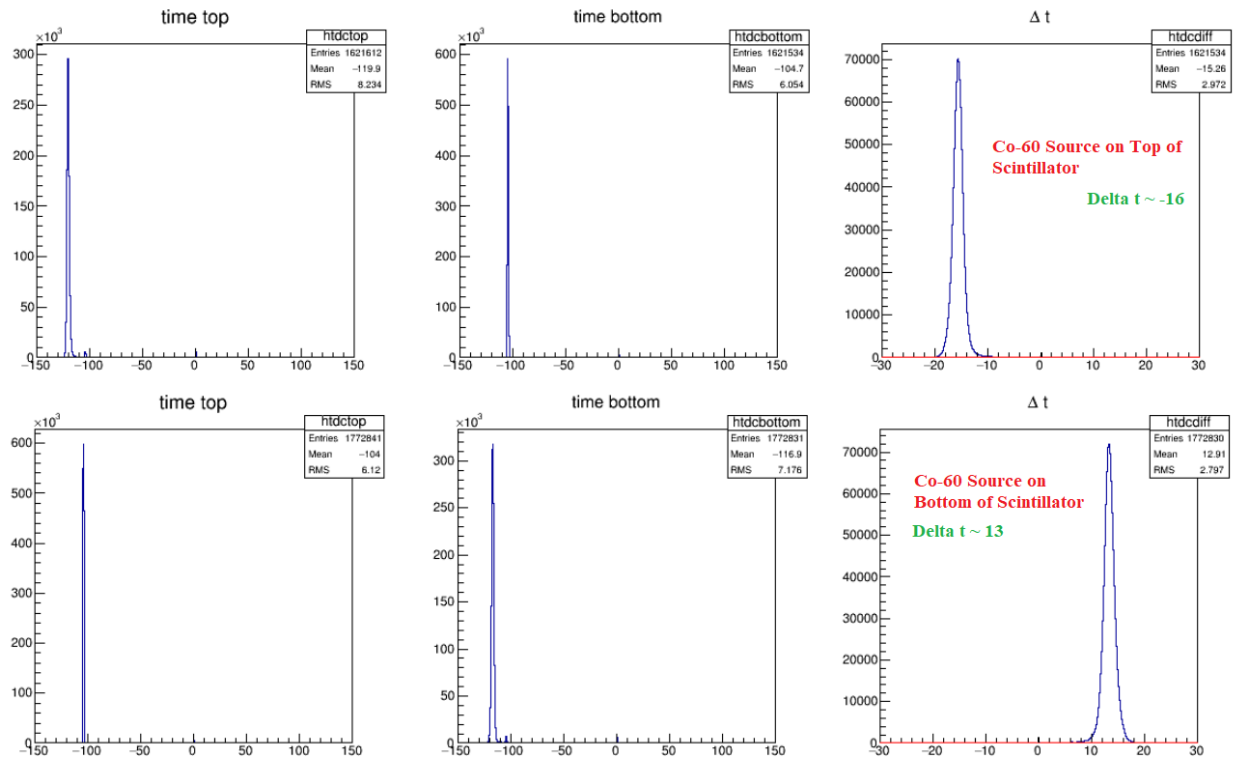


Figure 14 The timing signals for when Co-60 is placed on the scintillator bar. The top row shows the timing signals in the top PMT (far left), the bottom PMT (middle) and the difference between the two (far right) when the source is placed on the top of the scintillator. The bottom row shows the timing signals in the top PMT (far left), the bottom PMT (middle) and the difference between the two (far right) when the source is placed on the bottom of the scintillator.

For example, from figure 14, the difference in timing signals for the top is approximately -16 nanoseconds and the difference in timing signals for the bottom is approximately +13 nanoseconds. The total difference, then, is 29 nanoseconds. If the sources were placed 20 centimeters from the top and bottom of the scintillator bar, and the total length of the bar is 250 centimeters, then the photons will have to travel 20 cm from one PMT and 230 cm to the other pmt. The difference between the distances they must travel to reach either PMT is 210 centimeters. Simple physics allows the distance to be divided by the total timing signal to yield a function of position based on time of 7.24 centimeters per nanosecond traveled by the photons. This is how the Proton Veto Wall determines the location of a charged particle, and because the LANA sits directly behind it, the VW can inform LANA the approximate area where the charged particle will land and LANA can ignore its signal as it obviously comes from the charged particle coming from the reaction at the target position.

Preliminary Results

Preliminary results show that the Proton Veto Wall functions exactly as it should. The detector vetoes over billions of charged particle signatures from the LANA while keeping track of the energy of charged particles as they pass through the VW. Figure 15 shows the spectra of all detected charged particles before the VW is activated while figure 16 shows the spectra of all detected charged particles after the VW is activated. Notice that when the VW is activated, only the charged particles that are a direct result of proton recoil in the LANA are detected. In figure 15, charged particles dominated the spectra. When vetoing occurs, these charged particles (most evident in the green band) disappear.

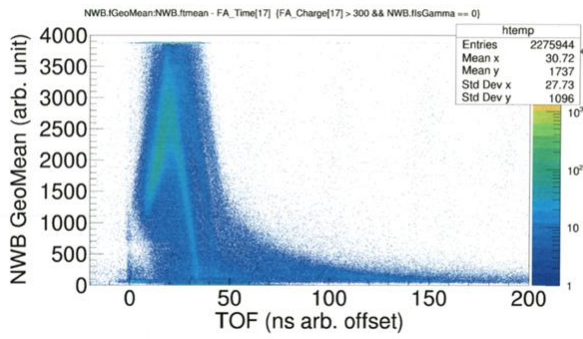


Figure 15 The LANA spectra before the VW is activated.

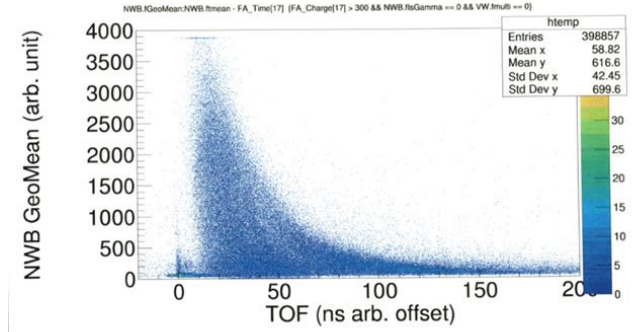


Figure 16 The LANA spectra after the VW is activated.

Figures 15 and 16 show the time (in nanoseconds) it takes the particles to reach the LANA (beginning when the particle is emitted from the heavy ion collision) on the x-axis and the energy (in arbitrary units) deposited into the LANA on the y-axis. Higher energy particles will have a lower time of flight (TOF) because they reach the detector much sooner (a high kinetic energy corresponds to a high velocity). These high energy particles also deposit much less energy in the detectors because they are able to more easily penetrate the material at higher speeds.

Acknowledgements

I would like to thank my professor, mentor, and thesis advisor Doctor Zbigniew Chajecki for his unwavering patience and support these last three years and for providing me with the opportunity to perform undergraduate research in experimental nuclear physics. I would also like to thank the Lee Honors College, Office of the Vice President for Research, the College of Arts and Sciences, and the Physics Department at WMU for funding and advising during my time as an undergraduate at the university. A special thank you to Michigan State University for allowing me access to their amazing facility: the National Superconducting Cyclotron Laboratory. Finally I would like to thank the other undergraduate and graduate students who helped me along my journey: Jaclyn Brett, Om Khanal, and Cordero Soto. Without them, none of the progress I made would have been possible.

References

- Coupland, D. D. (2013). *Probing the Nuclear Symmetry Energy with Heavy Ion Collisions* (Doctoral dissertation, Michigan State University, Lansing).
- Danielewicz, P., Lynch, W. G., & Lacey, R. (2002, November 22). Determination of the Equation of State of Dense Matter [Electronic version]. *Science*, 298(5598).
- Hoyle, F. (1975). *Astronomy and Cosmology a Modern Course* (p. 339). N.p.: W.H. Freeman and Company.
- Knoll, G. F. (n.d.). *Radiation Detection and Measurement* (4th ed.). 2010: Wiley.
- Prekeges, J. (2011). *Nuclear Medicine Instrumentation* (pp. 17-27). Sudbury, MA: Jones and Bartlett Publishers.
- Scintillators (2009). In *Stanford: Advanced Optical Ceramics Laboratory*. Retrieved April 25, 2018.
- "Scintillation Detectors." *Scionix*. Accessed 27 Apr. 2018.
- Taylor, J. R., Zafiratos, C. D., & Dubson, M. A. (2015). *Modern Physics for Scientist and Engineers* (2nd ed., pp. 412-425). Mill Valley, CA: University Science Books.
- Vancleave, J. (2011, March 8). Fluorescence vs. Phosphorescence. In *Vancleave's Science Fun*. Retrieved April 26, 2018.
- Yoo, Wook Jae & Hun Shin, Sang & Eun Lee, Dong & Jang, Kyoung & Cho, Seunghyun & Lee, Bongsoo. (2015, August). Development of a Small-Sized, Flexible, and Insertable Fiber-

Optic Radiation Sensor for Gamma-Ray Spectroscopy. Sensors. 15. 21265-21279.

10.3390/s150921265.